Physica C: Superconductivity and its applications 550 (2018) 19–26

Contents lists available at ScienceDirect

Physica C: Superconductivity and its applications

journal homepage: www.elsevier.com/locate/physc

Temperature behavior of the magnetoresistance hysteresis in a granular high-temperature superconductor: Magnetic flux compression in the intergrain medium

S.V. Semenov*, D.A. Balaev

Kirensky Institute of Physics, Federal Research Center KSC SB RAS, Krasnoyarsk 660036 Russia

A B S T R A C T

Granular high-temperature superconductors (HTSs) are characterized by the hysteretic behavior of magnetoresistance. This phenomenon is attributed to the effective field in the intergrain medium of a granular HTS. At the grain boundaries, which are, in fact, weak Josephson couplings, the dissipation is observed. The effective field in the intergrain medium is a superposition of the external field and the field induced by magnetic moments of HTS grains. Meanwhile, analysis of the field width of the R(H) magnetoresistance hysteresis $\Delta H = H_{dec} - H_{inc}$ at H_{dec} = const, where H_{inc} and H_{dec} are increasing and decreasing branches of the R(H) hysteretic dependence, shows that the effective field in the intergrain medium exceeds by far both the external field and the field induced by magnetic moments of HTS grains. This situation suggests the magnetic flux compression in the intergrain medium because of the small length of grain boundaries, which amounts to ~1 nm, i.e., is comparable with the coherence length and corresponds to Josephson tunneling in HTS materials. In this work, using the previously developed approach, we examine experimental data on the magnetoresistance and magnetization hysteresis in the granular $YBa_2Cu_3O_7$ HTS compound in the range from 77 K to the critical temperature. According to the results obtained, the degree of magnetic flux compression determined by the parameter α in the expression for the effective field $B_{eff}(H) = H - 4\pi M(H) \alpha$ in the intergrain medium remains constant over the investigated temperature range. All the features of the observed evolution of the R(H) hysteretic dependences are explained well within the proposed approach when the expression for $B_{eff}(H)$ contains the experimental M(H) magnetization data and the parameter α of about 20–25. The latter is indicative of the dominant effect of magnetic flux compression in the intergrain medium on the transport properties of granular HTS materials.

1. Introduction

Granular superconductors can be considered, in terms of their magnetic and transport properties, as materials consisting of two subsystems with different superconducting parameters: grains with the strong first and second critical fields H_{C1} and H_{C2} and high critical current densities J_C and grain boundaries with the much lower H_{C1} and J_C values [1–4]. These two subsystems exhibit the strong and weak superconductivity, respectively. The magnetic properties of granular superconductors are determined by grains (the currents circulate inside grains), whereas the macroscopic critical current of bulk samples is specified by the grain boundaries [3–5]. In the latter subsystem, the superconducting current is transferred from one grain to another through the grain boundary by means of Josephson tunneling. This tunneling, in turn, can be implemented when the geometric length of the grain boundaries is comparable with the coherence length of superconducting grains. This situation is implemented in granular HTS materials, where the above-mentioned quantities have the same order of magnitude and are no more than several nanometers [5–9].

The two above-mentioned subsystems manifest themselves differently in the magnetic and transport measurements of granular HTS systems. The external field is fully screened to the H_{C1} value that corresponds to the intergrain boundary subsystem; after that, in a certain field range, one can observe the magnetic hysteresis typical of this subsystem [3,4,10]. However, this field range is narrow (tens of Oersted at the liquid helium temperature) and decreases with temperature; at nitrogen temperatures, it amounts to several fractions of Oersted [3,4,6,10]. At the same time, the M(H) magnetic hysteresis loops observed by standard techniques in moderate and strong fields [11–14] are mainly caused by the response of the HTS grain subsystem; the data on the magnetic hysteresis loop are used to obtain the functional dependences of the intragrain critical current. The resistive transition of

* Corresponding author.
E-mail address: svsemenov@iph.krasn.ru (S.V. Semenov).

https://doi.org/10.1016/j.physc.2018.04.005
Received 10 January 2018; Received in revised form 27 February 2018; Accepted 13 April 2018
Available online 14 April 2018
0921-4534/

granular HTS materials in the external magnetic field occurs in two stages: first, as the temperature decreases, the transition of the HTS grain subsystem to the superconducting state occurs; then, the gradual transition in the subsystem of intergrain boundaries is observed [15–27].

However, the investigated subsystems interact with each other; specifically, when a superconductor is placed in the external field, the magnetic moments of HTS grains affect the resulting field in the intergrain boundaries [28,29]. This leads to the observed magnetoresistance hysteresis R(H) at T = const [30–38]. Moreover, in view of the small geometrical length of the intergrain boundaries, the magnetic flux lines in them are crowded [28,29] and the degree of this crowding can be fairly high [33]. Previously [39], we presented a method for determining the effective field in the intergrain medium, i.e., the degree of magnetic flux crowding. The aim of this study was to follow the temperature evolution of the degree of magnetic flus crowding in the intergrain medium of a granular HTS material on the basis of the R(H) and M(H) experimental data.

The paper is organized as follows. In Section 2, we briefly review the concepts of a two-level model (intergrain boundaries and grains) and internal mechanisms responsible for the observed magnetoresistance hysteresis R(H). In addition, we explain the examined magnetic field compression in the intergrain medium. Section 3 contains the experimental part; it is noteworthy that the investigated $YBa_2Cu_3O_7$ material represents a standard sample prepared using the solid-state synthesis technique. In Section 4, we illustrate a method for determining the flux crowding parameter and analyze the experimental data obtained. Section 5 presents conclusions. In our opinion, the established weak temperature dependence of the degree of flux crowding is not a characteristic of a specific investigated sample, but a feature of the granular HTS materials, at least, those belonging to the yttrium system.

2. Brief review of the magnetotransport properties of granular HTS materials and model justification

The existence of the two subsystems in granular HTS materials manifests itself, first of all, in the transport properties of as a two-step resistive transition [15–27] (see Fig. 1; the data presented in Figs. 1 and 2 were obtained on the investigated $YBa_2Cu_3O_7$ sample and are presented in Introduction as an illustration). The sharp jump of resistance R corresponds to the superconducting transition in HTS grains, while

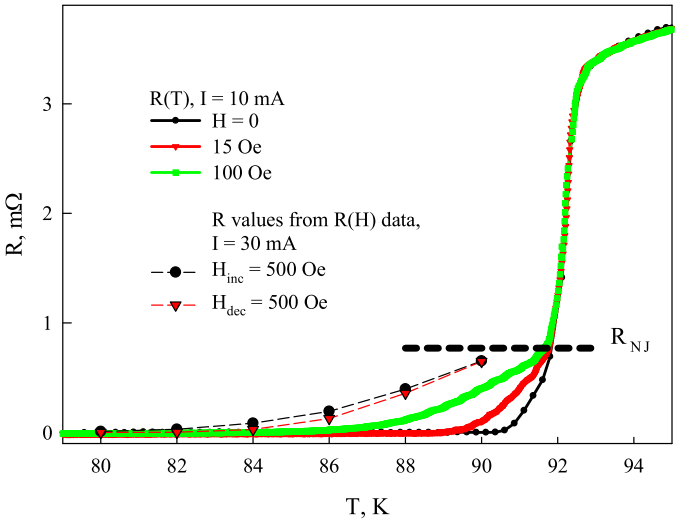

Fig. 1. Temperature dependences of the resistance R(T) for the investigated $YBa_2Cu_3O_7$ sample at different external fields and data obtained from the R(H) dependences in increasing (H_{inc}) and decreasing (H_{dec}) fields of 500 Oe. The dashed horizontal line shows the contribution R_{NJ} of grain boundaries to the total sample resistance.

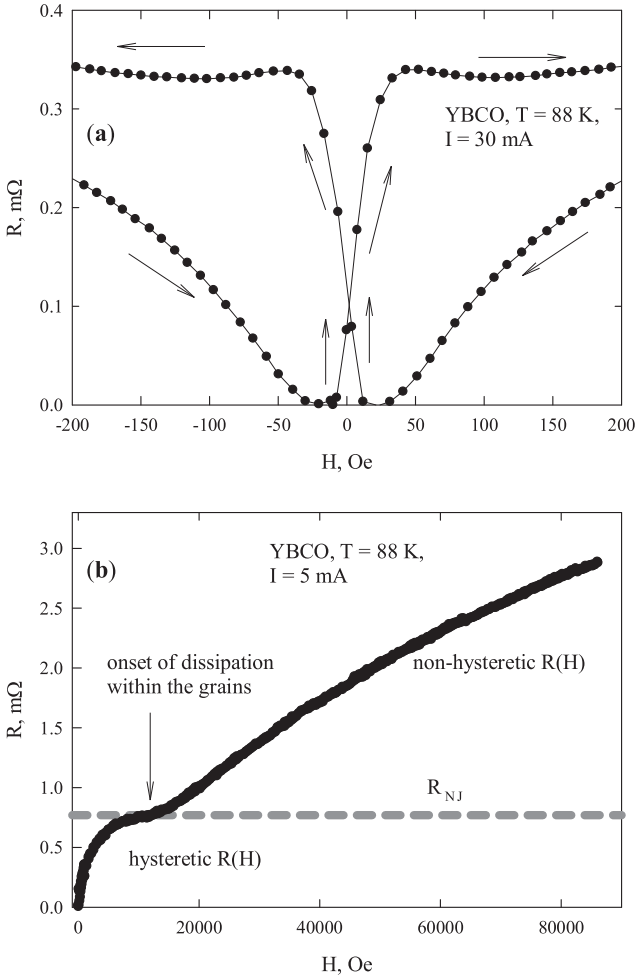

Fig. 2. Magnetoresistance R(H) of the investigated $YBa_2Cu_3O_7$ sample (T = 88 K). (a) Low-field portion of the R(H) hysteretic dependence; arrows show the external field variation direction. (b) R(H) dependence in fields of up to 90 kOe; the regions of existence (absence) of the hysteresis and the field of the dissipation onset in HTS grains are shown. The dashed horizontal line shows the contribution R_{NJ} of grain boundaries to the total sample resistance in accordance with the data presented in Fig. 1.

the smooth portion of the R(T) dependence reflects the transition in the subsystem of grain boundaries. It is worth noting that, according to the numerous data, the increase in the magnetic field and transport current does not change the resistance of the smooth R(T) portion denoted in Fig. 1 as R_{NJ} [15–27]. This quantity can be considered to be the normal resistance of the grain boundaries (or their contribution to the resistance right above the superconducting transition).

Another specific feature of the transport properties of granular HTS materials is the hysteresis of magnetoresistance isotherms R(H), which is illustrated in Fig. 2a. Note the main experimental peculiarities of the hysteretic behavior of the R(H) dependences [30–42]. The resistance in the increasing external magnetic field H_{inc} is higher than the resistance of the decreasing external field H_{dec}: $R(H_{inc}) > R(H_{dec})$. The exception is the behavior in the vicinity of H = 0. The shape of the R(H) curves strongly depends on the transport current, in view of nonlinearity of the I–V characteristics. In relatively weak fields (100–200 Oe) at sufficiently high temperatures, one can observe a local minimum of the R(H_{inc}) dependence, as well as the R(H_{dec}) minimum. These peculiarities take place in the external field range where the observed dissipation only occurs in the subsystem of grain boundaries, while in sufficiently strong fields, when the R(H) dependence forms a plateau at $R \approx R_{NJ}$, one can observe the sharp growth of the electrical resistance, which is

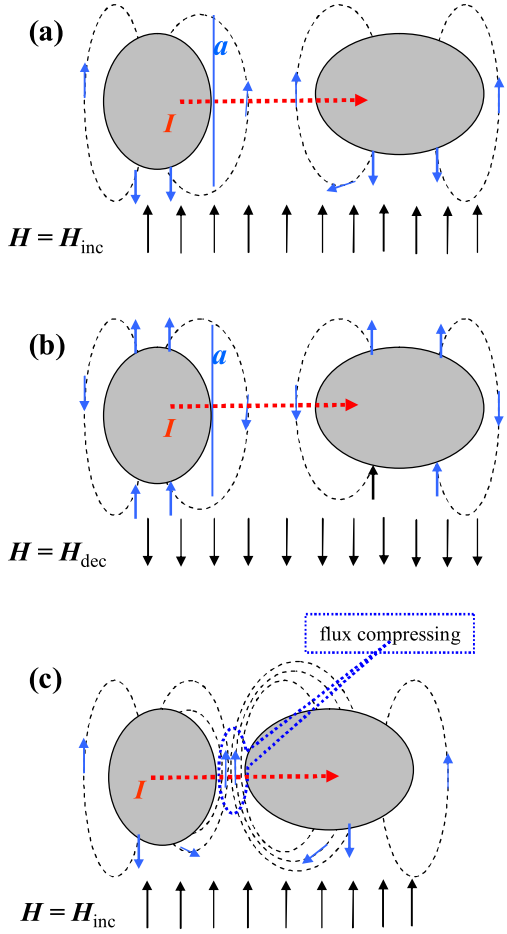

Fig. 3. Schematic of magnetic flux lines in the intergrain medium of a granular HTS. Upward and downward vertical arrows show the directions of (a, c) increasing and (b) decreasing external field and dashed lines, the magnetic flux lines induced by the magnetic moments of HTS grains (ovals). Dotted lines show the direction of microscopic current ***I*** for the idealized picture at $\boldsymbol{H} \perp \boldsymbol{j}$ ($\boldsymbol{j}$ is the macroscopic current); $\boldsymbol{a}$ is the grain boundary plane ($\boldsymbol{I} \perp \boldsymbol{a}$). (c) Schematic explaining the effect of magnetic flux compression in the intergrain spacings in the case of grains close to each other.

related to the transition to the resistive (mixed) state of superconducting grains (Fig. 2b). In this field range, the R(H) hysteresis is not observed [34,40,41].

The above-mentioned experimental fact $R(H_{inc}) > R(H_{dec})$ is actually the clockwise hysteresis, which allowed to suggest that the grain boundaries are located in some effective field, which is a superposition of the external field and the field induced by magnetic moments of superconducting grains [28,43,33]. Fig. 3 shows a schematic of the field distribution in the grain boundaries at $H = H_{inc}$ (Fig. 3a) and $H = H_{dec}$ (Fig. 3b) with regard to the fact that the magnetization hysteresis M(H) is typical of type-II superconductors: $M(H_{inc}) < M(H_{dec})$ and $M(H_{inc}) < 0$. In the case illustrated in Fig. 3, the external field is perpendicular to the microscopic current I ($\boldsymbol{H} \perp \boldsymbol{I}$) and the effective field B_{eff} in the region of carrier tunneling can be written in the form

$$B_{eff} = H - 4\pi M \alpha. \quad (1)$$

Here, we took into account the sign of sample magnetic moment, which is directed opposite to the external field at $H = H_{inc}$, and reasonably suggested that, instead of magnetic moments of grains, we can use the experimental magnetic hysteresis loop M(H) of the sample. The coefficient of proportionality α in Eq. (1) takes into account the effect of demagnetizing factors of grains and magnetic flux compression (see below) in the intergrain spacings.

According to the commonly accepted concepts, the dissipation in type-II superconductors can be described by the Arrhenius relation [44]

$$R \sim \exp(-U_P(H, T, j)/k_B T), \quad (2)$$

where $U_P(H, T, j)$ is the dependence of the pinning potential on magnetic field, temperature, and transport current (k_B is the Boltzmann constant). Eq. (2) is applicable to the subsystem of grain boundaries, but, certainly, in this case, the H value in Eq. (2) is replaced by B_{eff}, or, more exactly, its absolute value ($|B_{eff}| \rightarrow H$). It was found that this approach explains well the above-mentioned features of the R(H) hysteretic dependence (clockwise hysteresis $R(H_{inc}) > R(H_{dec})$) [38–40] and nonmonotonic behavior of the $R(H_{inc})$ and $R(H_{dec})$ dependences [31,45,39,46]). This approach is also applicable to the description of transport $J_C(H)$ hysteretic dependence. So far as $R \sim 1/J_C$, the $J_C(H)$ is a "mirror image" of R(H) dependence (measured at a constant current $I > I_C$). The $J_C(H)$ dependence demonstrates anticlockwise hysteresis [28,43,34,46–49].

Obviously, at the sufficiently large intergrain spacings (Fig. 3a and b), the α value will be comparable with the demagnetizing factor of a grain. However, if we "bring" two grains close to each other (Fig. 3c) to an intergrain distance of about 1 nm, as in granular materials, then, the magnetic flux lines will undoubtedly be crowded in the intergrain region and, consequently, the α value will increase. The assumption about the significant magnetic flux compression in the intergrain medium of a granular HTS material was formulated first in [33]. Indeed, comparison of the experimental R(H) and M(H) hysteretic dependences [39], including the relaxation R(H = const, t) and M (H = const, t) dependences, and the R(H) and M(H) hysteresis at different external field variation rates [51] using Eq. (1) showed that the α value is much larger than unity, which confirms the above hypothesis. Thus, the intergrain medium of a granular HTS is located in the effective field B_{eff} determined by Eq. (1) and the parameter α characterizes the degree of magnetic flux compression in the intergrain medium.

In addition, it is well-known that the magnetoresistive effect in granular HTS materials is anisotropic with respect to the mutual orientation of the magnetic field and transport current: $R(\boldsymbol{H} \perp \boldsymbol{j}) > R(\boldsymbol{H} \,||\, \boldsymbol{j})$ [22,33,20]. This anisotropy reflects the fact that the magnetoresistance is determined by the projection of vector $\boldsymbol{B}_{eff}$ onto the grain boundary plane $\boldsymbol{a}$ (Figs. 3a and 3b); i.e., the dissipation is maximum when the microscopic current $\boldsymbol{I}$ is perpendicular to $\boldsymbol{B}_{eff}$ [33]. As a result, in magnetoresistive measurements, the flux compression is the most pronounced at the perpendicular orientation $\boldsymbol{H} \perp \boldsymbol{j}$ [51]. In [52], we obtained a value of $\alpha \approx 22$ for a granular HTS sample of the classical yttrium system at $\boldsymbol{H} \perp \boldsymbol{j}$.

Note that in all the above-cited studies [45,46,39,50–52] the parameter α of the yttrium or bismuth HTS systems was obtained from the R(H) and M(H) data obtained at the liquid nitrogen temperature. In view of this, the question about temperature evolution of the parameter α arises. In other words, it is necessary to clarify whether the α value (Eq. (1)) reflecting the flux compression in the intergrain spacings will change at low temperatures or in the vicinity of T_C. In our opinion, such investigations would advance the understanding of the described flux compression effect on the dissipation processes in granular HTS materials at different temperatures. For this purpose, here we determine the α values by comparing the R(H) and M(H) hysteretic dependences measured at different temperatures on a granular HTS with the classical $YBa_2Cu_3O_7$ composition.

3. Experimental

The $YBa_2Cu_3O_7$ (YBCO) sample was prepared by a standard solid-state synthesis technique from the corresponding oxides at temperatures of 900–920 °C with three intermediate grindings. According to the X-ray diffraction data, the synthesized HTS sample had the 1-2-3 structure without visible foreign phases. The grain size determined by scanning electron microscopy was ~ 6 μm. The magnetic

measurements in weak magnetic fields revealed a superconducting transition temperature of 92 K, which is consistent with the R(T) data (Fig. 1). The critical current determined using the criterion 1 μV/cm at a temperature of 77 K in zero external magnetic field was found to be 150 A/cm^2.

The transport properties, including magnetoresistance (R(H) dependences), were measured by a standard four-probe technique. The samples were about 1 × 1 × 6 mm^3 in size. Pressed gold-plated electric contacts to the sample ensured the low contact resistance. In such measurements performed at temperatures from 77 K, the magnetic field was induced by an electromagnet. In the R(H) and R(T) measurements (the resistance R was determined as a voltage drop divided by the transport current *I*), the sample was cooled in zero external field. The R(H) measurements at 77 K and transport currents of 30–150 mA were performed on the samples immersed directly in a cryogenic liquid (liquid nitrogen). The measurements at temperatures above 77 K were performed at a transport current of 30 mA; in this case, the sample was in the helium atmosphere at the stabilized temperature. It was observed that the transport current $I = 30$ mA used in the measurements of the temperature evolution of the R(H) dependences did not lead to the sample heating. It is worth noting that in the R(H) measurements, the external field was from H = 0 to $H_{max} = 1000$ Oe. Then, the external field changed cyclically to $-H_{max}$, $+H_{max}$ and, after that, to H = 0. The R(H) dependences were analyzed for a loop within $-H_{max}$ $+H_{max}$, excluding the virgin curve from H = 0 to H_{max}. The R(T) dependences obtained in different external fields under zero-field cooling conditions (Fig. 1) correspond to a transport current of $I = 10$ mA. The R(H) dependence in fields of up to 90 kOe at T = 88 K (Fig. 2b) was obtained on a Physical Property Measurement System PPMS-6000 (Quantum Design) at a transport current of $I = 5$ mA.

The hysteretic magnetization dependences were obtained on a vibrating sample magnetometer [53] on the sample used in the transport measurements. In all the R(H) and M(H) measurements performed at different temperatures, the external field variation rate dH/dt ≈ 10 Oe/s and thermomagnetic prehistory of the samples were the same.

4. Results and discussion

4.1. Temperature evolution of the R(H) dependences

Fig. 4 shows the R(H) dependences measured at different temperatures in the maximum applied field of $H_{max} = 1000$ Oe. These dependences, together with the data presented in Fig. 2a, show that the R(H) hysteresis features described in Section 2 evolve upon temperature variation. The field H_{inc} at which the R(H_{inc}) dependence has a local maximum in weak fields decreases with increasing temperature. On the other hand, as the temperature increases, the field range where the R(H_{dec}) values become almost zero (for comparison, see Fig. 2a) narrows and at $T = 90$ K, the R(H_{dec}) dependence has the minimum in the vicinity of $H_{dec} \approx 10$ Oe. The position of the R_{NJ} value, i.e., the normal resistance of the grain boundaries, is always higher than the R(H) dependence (see Fig. 1, which shows the resistances in a field of 500 Oe for the increasing and decreasing field obtained from the R(H) dependences). Only in fairly strong fields, one can observe a peculiarity, i.e., the change in the curvature sign of the R(H) dependence (Fig. 2b; H ≈ 12 kOe and $T = 88$ K), at which the magnetoresistance of the subsystem of grain boundaries saturates; after that, the dissipation starts in the subsystem of superconducting grains with an increase in the field.

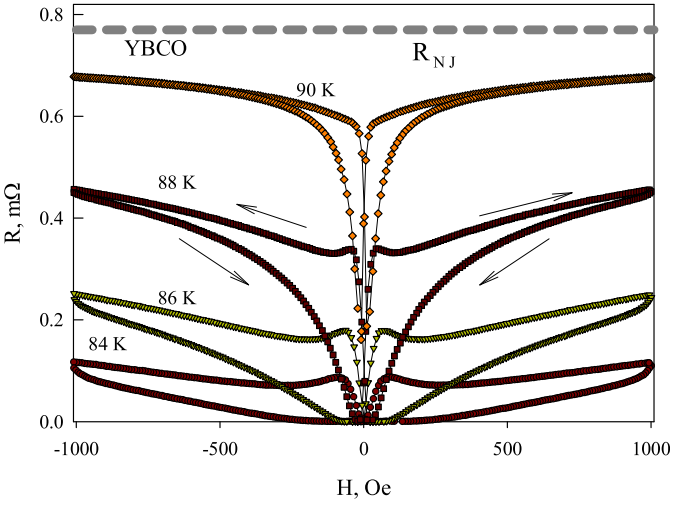

Fig. 4. Experimental R(H) dependences for the investigated sample at different temperatures. Arrows show the external field variation direction. The dashed horizontal line corresponds to the contribution R_{NJ} of the grain boundaries to the total sample resistance, according to the data presented in Fig. 1.

According to Eq. (1), to establish the effective field B_{eff}(H) in the intergrain medium and analyze the R(H) hysteresis, we should operate with the sample magnetization M(H). The M(H) magnetic hysteresis loops under the experimental conditions analogous to the conditions of the R(H) measurements are presented in Fig. 5. Note that the shape of M(H) curves is typical of the granular yttrium HTS system [54].

4.2. R(H) dependences at different transport currents. Field width of the magnetoresistance hysteresis

Fig. 6a shows the R(H) dependences measured at $T = 77$ K and different transport currents. It can be seen that, in view of the strong nonlinearity of the *I–V* characteristics, the shape of the R(H) dependences changes with increasing current: the resistance at H = const increases and the field range with R(H_{dec}) ≈ 0 narrows. Nevertheless, as we showed previously [55,56], the family of R(H) hysteretic dependences obtained at T = const and different currents I is characterized by the transport current-independent parameter: magnetic-field width of the hysteresis ΔH. It is reasonable to define this quantity as $\Delta H = H_{dec} - H_{inc}$ at R = const [55,56,39,41,52]. Fig. 6a shows the example of determination of this quantity at $H_{dec} = 900$ Oe, where the length of horizontal lines is, in fact, the field width of the hysteresis and the vertical lines correspond to $H_{dec} = 900$ Oe and $H_{inc} = 60$ Oe. The identical H_{inc} values at the same H_{dec} value evidence for the transport current-independent field width of the hysteresis ΔH (at $H_{dec} = 900$ Oe, we have ΔH ≈ 840 Oe).

Indeed, according to Eq. (2), the magnetoresistance R is determined

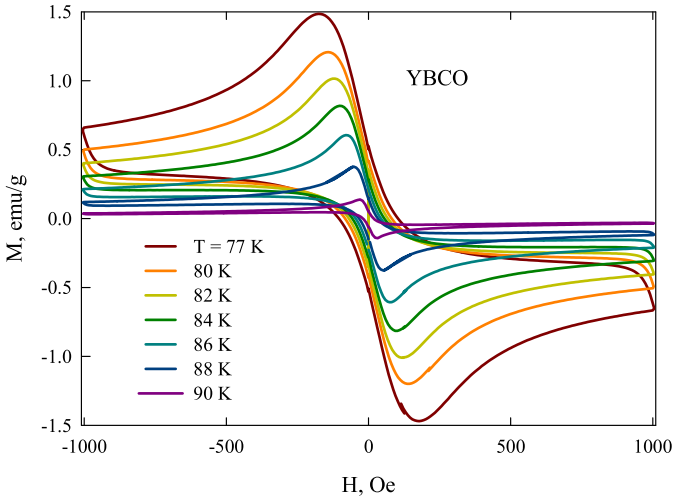

Fig. 5. Experimental M(H) dependences for the investigated sample at different temperatures.

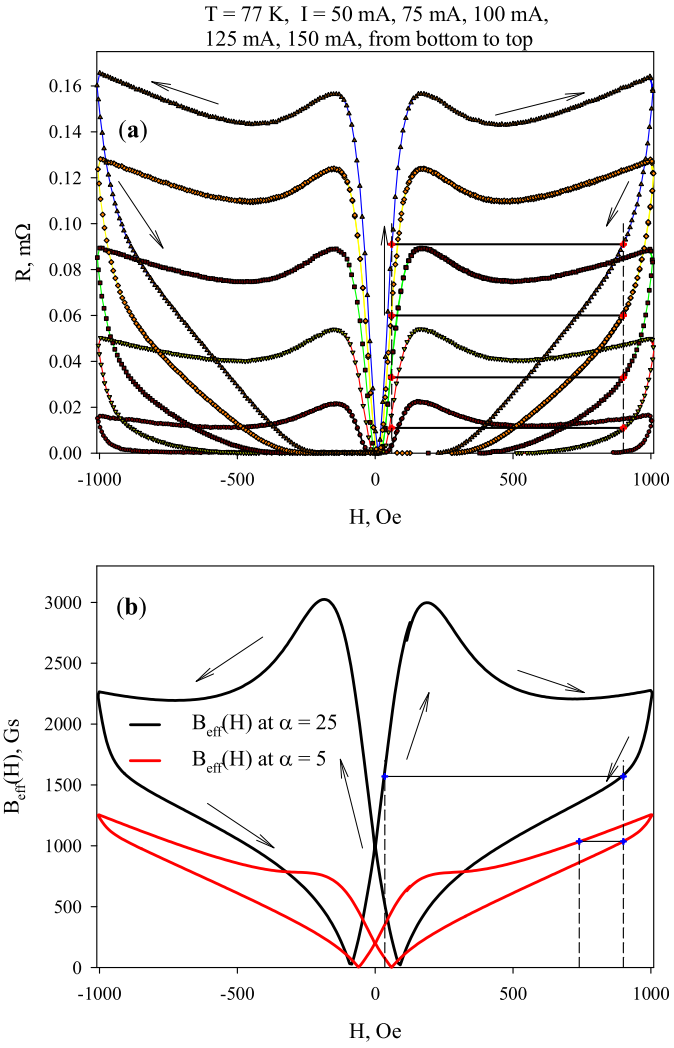

Fig. 6. (a) Experimental R(H) dependences of the investigated sample $YBa_2Cu_3O_7$ at a temperature of 77 K and different currents *I*. Horizontal lines show the field width of the hysteresis ΔH at H_{dec} = 900 Oe; their equal lengths indicate the independence of the ΔH value of the transport current at *T* = const and H_{dec} = const. The dashed horizontal line shows the contribution R_{NJ} of the grain boundaries to the total sample resistance in accordance with the data presented in Fig. 1. (b) Hysteretic dependences of the effective field in the intergrain medium calculated from the M(H) data using Eq. (1) at a temperature of 77 K and α values given in (b). Horizontal lines in (b) show the field width of the hysteresis ΔH for the B_{eff}(H) dependences at H_{dec} = 900 Oe. Arrows in (a) and (b) show the external field variation direction.

by the effective field B_{eff} in the intergrain medium: R ~ B_{eff}. Hence, at R(H_{dec}) = R(H_{inc}) (the condition for determining the ΔH value), the effective fields at H = H_{dec} and H = H_{inc} are equal as well: $B_{eff}(H_{dec}) = B_{eff}(H_{inc})$. We write this condition using the right-hand side of Eq. (1) and taking into account that the magnetization and effective field are functions of the external field H:

$$H_{dec} - 4\pi M(H_{dec})\alpha = H_{inc} - 4\pi M(H_{inc})\alpha.$$

Using this expression, we can easily determine the field width of the hysteresis ΔH

$$\Delta H = H_{dec} - H_{inc} = 4\pi\alpha\,[M(H_{dec}) - M(H_{inc})]. \quad (3)$$

It can be seen that the field width of the hysteresis only depends on the magnetizations M(H_{inc}) and M(H_{dec}) and parameter α, which characterizes the degree of magnetic flux compression in the intergrain medium. It is worth noting that the independence of ΔH of the current confirms that the magnetization of the subsystem of grain boundaries does not contribute to the observed R(H) hysteresis [55,56] (otherwise, the current variation could affect the magnetization of this subsystem [55]).

4.3. Determining the degree of magnetic flux compression in the intergrain medium

It follows from Section 4.2. that the field width of the hysteresis can serve a current-independent parameter determined by the experimental M(H) dependence and degree of flux compression in the intergrain medium, i.e., parameter α, which can be considered, in the first approximation, to be independent of field H [39,50,52]. The only unknown parameter in Eq. (3) is α. It can be determined by comparing the field width of the R(H) hysteresis and field width of the B_{eff}(H) hysteresis in the intergrain medium (Eq. (1)) with the use of the experimental M(H) data.

The B_{eff}(H) hysteretic dependences in Fig. 6b were built at the two α values from the M(H) data presented in Fig. 5 at T = 77 K. Note that these dependences are very similar to the R(H) dependences in shape and, in addition, reflect all the peculiarities of the experimental R(H) dependences, $B_{eff}(H_{inc}) > B_{eff}(H_{dec})$, except for the portion in the vicinity of H = 0, the local R(H_{inc}) maximum, and the R(H_{dec}) minimum. In addition, comparison of the field widths of the R(H) and B_{eff}(H) hysteresis (ΔH is the length of the horizontal straight lines in Fig. 6a and b, respectively, at H_{dec} = 900 Oe) shows that only at the sufficiently large parameter α (α = 25) we can obtain similar hysteresis widths (compare with ΔH, i.e., the length of a segment at α = 5 in Fig. 6b).

Fig. 7 illustrates the detailed comparison of the hysteretic dependences of the field width of the R(H) and B_{eff}(H) hysteresis by the example of the data obtained at a temperature of *T* = 82 K. Fig. 7a presents simultaneously the R(H) (the R axis on the left) and B_{eff}(H) (the B_{eff} axis is on the right) hysteretic dependences at α = 25. The abscissas of points A, B, and C correspond to the values of H_{dec} = 980, 900, and 600 Oe. Points A′, B′, and C′ correspond to the crossings of the horizontal straights AA′, BB′, and CC′ with the R(H_{inc}) dependence; i.e., the lengths of segments AA′, BB′, and CC′ determine the field widths of the R(H) hysteresis at the given H_{dec} values. At the same time, the lengths of segments AA″, BB″, and CC″ correspond to the field width of the B_{eff}(H) hysteresis. It can be seen from Fig. 7a that the abscissas of the pairs of points (A′, A″), (B′, B″), and (C′, C″) are almost identical (shown in Fig. 7a by the dashed vertical lines), i. e., the lengths of segments AA′ and AA″, BB′ and BB″, and CC′ and CC″ are almost the same. This is obtained at α = 25.

The agreement between the segment lengths is broken when the smaller α value is taken. Comparison of the R(H) and B_{eff}(H) hysteretic dependences at α = 15 is illustrated in Fig. 7b. The abscissas of points C′ and C″ are similar, whereas the abscissas of the pairs of points A′, A″ and B′, B″ are strongly different.

The R(H) and B_{eff}(H) hysteresis (Fig. 7) allows us to determine the dependences of ΔH on H_{dec}, $\Delta H(H_{dec}) = H_{dec} - H_{inc}$, at different H_{dec} values and R = const. For the sake of simplicity, we do not consider the two-valuedness of the ΔH(H_{dec}) dependence, which is observed due to the presence of a local minimum in the R(H_{inc}) and B_{eff}(H_{inc}) dependences. As a result, instead of the two-valuedness of the ΔH(H_{dec}) function in the range from H_{max} to some value H*, which corresponds to the R(H_{inc} = H*) (or B_{eff}(H_{inc} = H*)) minimum, there is a sharp jump of the ΔH(H_{dec}) function (Fig. 8) at H = H*. Fig. 8 shows the ΔH(H_{dec}) values obtained from the experimental dependences of the R(H) hysteresis (symbols) and the ΔH(H_{dec}) values obtained from the B_{eff}(H_{dec}) dependences calculated using Eq. (1) from the experimental M(H) data (Fig. 5) at a temperature of *T* = 82 K for the α values presented in Fig. 8. It can be seen that the best agreement for the wide external field range is obtained at α = 20–25.

Similarly, we processed the data obtained at different temperatures in the range from 77 K to T_C. For this purpose, we calculated the ΔH (H_{dec}) dependences from the experimental R(H) dependences and the

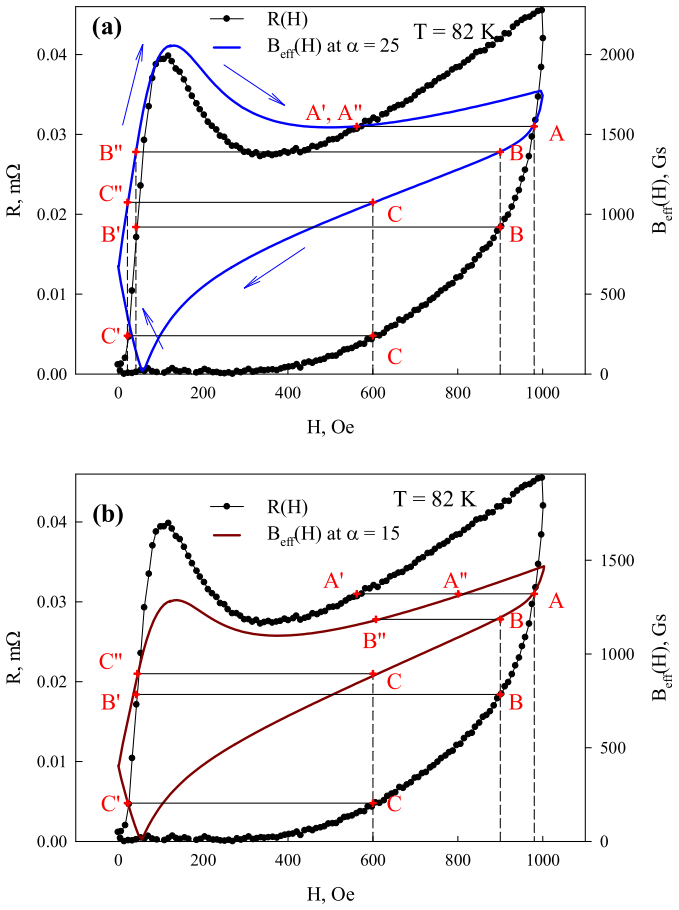

Fig. 7. R(H) (left-hand scale) and B_{eff}(H) (right-hand scale) hysteretic dependences at T = 82 K. Arrows show the external field variation direction. The B_{eff}(H) dependences are obtained using Eq. (1) from the M(H) data at T = 82 K and α values of (a) 25 and (b) 15. Horizontal lines show the field dependence of the hysteresis ΔH of the R(H) dependences (the lengths of segments AA′, BB′, and CC′) and B_{eff}(H) dependences (the lengths of segments AA″, BB″, and CC″) at H_{dec} = 980, 900, and 600 Oe (shown by the dashed vertical lines). Note (a) the almost identical lengths of segment pairs AA′ and AA″, BB′ and BB″, and CC′ and CC″ at α = 25 and (b) different segment lengths at α = 15. For more details, see Section 4.3.

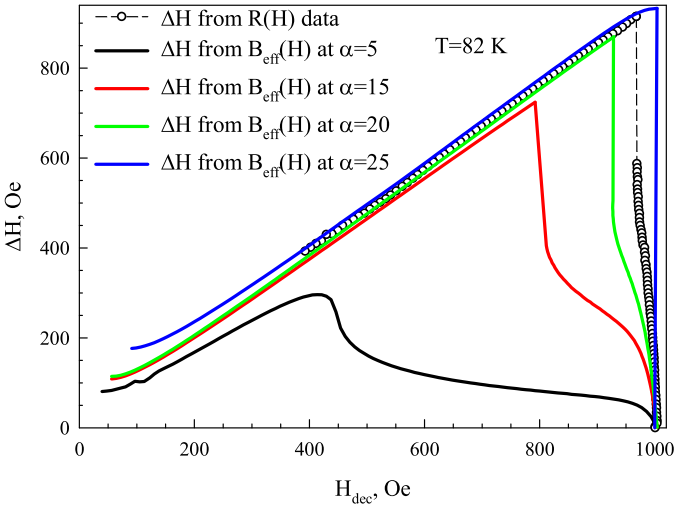

Fig. 8. Comparison of the field width of the ΔH(H_{dec}) hysteresis (symbols) for the experimental R(H) dependence at T = 82 K (see Fig. 7) with the calculated B_{eff}(H) dependences (lines) obtained from the M(H) data at T = 82 K (Fig. 5) using Eq. (1) at the given α values.

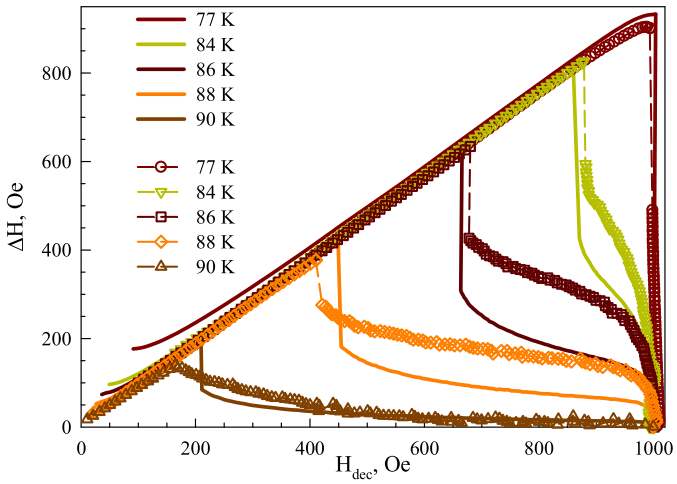

Fig. 9. Comparison of the field width ΔH(H_{dec}) of the hysteresis (symbols) for the experimental R(H) dependences at given temperatures with the calculated data (lines) for the B_{eff}(H) dependences obtained from the M(H) data at corresponding temperatures (Fig. 5) using Eq. (1) at α = 25.

ΔH(H_{dec}) dependences from the B_{eff}(H) hysteretic dependences; the M(H) data (Fig. 5) were taken for specific temperatures. Fig. 9 summarizes these data; symbols correspond to the ΔH(H_{dec}) dependences for the experimental R(H) curves and the lines, to the field width of the hysteresis obtained from the B_{eff}(H) dependence at α = 25. We obtained good agreement at all temperatures; the parameter α was the only fitting parameter.

Thus, we may state that the degree of magnetic flux compression in the intergrain medium, which is characterized by the parameter α in Eq. (1), remains almost invariable over the investigated temperature range and amounts to 20–25. The temperature evolution of the effective field in the intergrain medium as a function of the external field in the range from 77 K to T_C is illustrated in (Fig. 10, where the $|B_{eff}(H)|$ data are presented together with the $|B_{eff}|$ = H dependence with disregard of the flux compression. It can be seen that the effective field is always (even with a decrease in the field) stronger than the external field and this difference increases with decreasing temperature due to the growth of the diamagnetic response (Fig. 5).

5. Conclusions

Thus, we studied the evolution of the magnetoresistance hysteresis

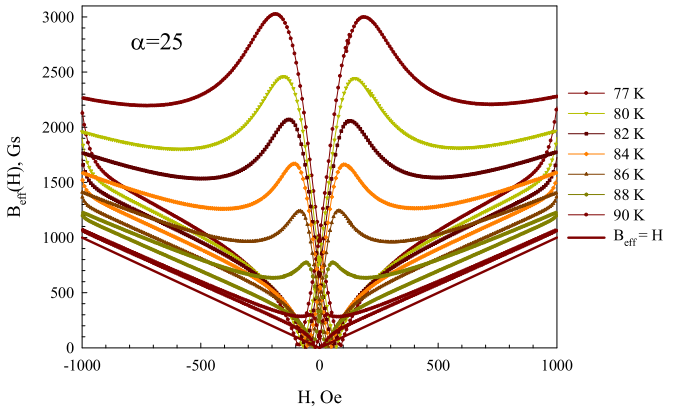

Fig. 10. Dependences of the effective field B_{eff}(H) in the intergrain medium obtained using Eq. (1) from the M(H) data (Fig. 5) at α = 25, which yields the best agreement between the field width of the hysteresis (Figs. 8 and 9) at given temperatures. For comparison, the linear dependence B_{eff} = H (external field) is shown.

R(H) of the granular $YBa_2Cu_3O_7$ HTS compound in the range from 77 K to the critical temperature. The R(H) hysteretic dependences were analyzed using the field width of the hysteresis $\Delta H = H_{dec} - H_{inc}$ under the condition $R(H_{dec}) = R(H_{inc})$, which is independent of the transport current. Based on the previously proposed concept of the effective field in the intergrain medium, which is related to the magnetization of a superconductor as $B_{eff}(H) = H - 4\pi M(H) \alpha$, we analyzed the experimental ΔH data and established the parameter α at different temperatures. We found this parameter to be α = 20–25 and almost *temperature-independent*. The obtained value is indicative of a significant flux compression in the intergrain medium, which is nearly constant over the investigated temperature range. As the temperature increases, the size of the M(H) hysteresis loop, magnetizations at the extremum points, and external fields corresponding to the M(H) extrema decrease. This affects the relative contribution of the second term ($-4\pi M(H) \alpha$) to the effective field and determines, according to (2) with $|B_{eff}(H)|$ replaced by H, the main features of the R(H) hysteretic dependence (its clockwise type and nonmonotonic behavior with a local maximum with an increase in the external field and a local minimum with a decrease in it) and its temperature evolution.

Acknowledgment

The work was supported by the Russian Science Foundation (Grant No. 17-72-10050).

References

[1] G. Wang, M.J. Raine, D.P. Hampshire, How resistive must grain boundaries in polycrystalline superconductors be, to limit J_C? Supercond. Sci. Technol. 30 (2017) 104001.
[2] L. Ji, M.S. Rzchowski, N. Anand, M. Tinkham, Magnetic-field-dependent surface resistance and two-level critical-state model for granular superconductors, Phys. Rev. B. 47 (1993) 470–483.
[3] J. Jung, M.-K. Mohamed, S.C. Cheng, J.P. Franck, Flux motion, proximity effect, and critical current density in $YBa_2Cu_3O_{7-\delta}$/silver composites, Phys. Rev. B. 42 (1990) 6181–6195.
[4] B. Andrzejewski, E. Guilmeau, C. Simon, Modelling of the magnetic behaviour of random granular superconductors by the single junction model, Supercond. Sci. Technol. 14 (2001) 904–909.
[5] P. Chaudhari, J. Mannhart, D. Dimos, C.C. Tsuei, J. Chi, M.M. Oprysko, M. Scheuermann, Direct measurement of the superconducting properties of single grain boundaries in $Y_1Ba_2Cu_3O_{7-\delta}$, Phys. Rev. Lett. 60 (1988) 1653–1656.
[6] E.B. Sonin, Josephson medium in high-temperature superconductivity: vortices and critical magnetic fields (theory), JETP Lett. 47 (1988) 496–499.
[7] D. Larbalestier, A. Gurevich, D.M. Feldmann, A. Polyanskii, High-Tc superconducting materials for electric power applications, Nature 414 (2001) 368–377.
[8] J.W.C. De Vries, G.M. Stollman, M.A.M. Gijs, Analysis of the critical current density in high-Tc superconducting films, Phys. C Supercond. 157 (1989) 406–414.
[9] M.I. Petrov, S.N. Krivomazov, B.P. Khrustalev, K.S. Aleksandrov, A study of the hysteresis property of the current-voltage characteristic in high-temperature superconductors, Solid State Commun 82 (1992) 453–456.
[10] F. Pérez, X. Obradors, J. Fontcuberta, X. Bozec, A. Fert, Magnetic flux penetration and creep in a ceramic $(Y,Sm)Ba_2Cu_3O_7$ superconductor, Supercond. Sci. Technol. 9 (1996) 161–175.
[11] A. Palau, T. Puig, X. Obradors, E. Pardo, C. Navau, A. Sanchez, A. Usoskin, H.C. Freyhardt, L. Fernández, B. Holzapfel, R. Feenstra, Simultaneous inductive determination of grain and intergrain critical current densities of $YBa_2Cu_3O_{7-x}$ coated conductors, Appl. Phys. Lett. 84 (2004) 230–232.
[12] E. Bartolomé, X. Granados, T. Puig, X. Obradors, E.S. Reddy, G.J. Schmitz, Critical state in superconducting single-crystalline $YBa_2Cu_3O_7$ foams: local versus long-range currents, Phys. Rev. B 70 (2004) 144514.
[13] D.M. Gokhfeld, D.A. Balaev, I.S. Yakimov, M.I. Petrov, S.V. Semenov, Tuning the peak effect in the $Y_{1-x}Nd_xBa_2Cu_3O_{7-\delta}$ compound, Ceram. Int. 43 (2017) 9985–9991.
[14] X.L. Zeng, T. Karwoth, M.R. Koblischka, U. Hartmann, D. Gokhfeld, C. Chang, T. Hauet, Analysis of magnetization loops of electrospun nonwoven superconducting fabrics, Phys. Rev. Mater. 1 (2017) 044802.
[15] M.A. Dubson, S.T. Herbert, J.J. Calabrese, D.C. Harris, B.R. Patton, J.C. Garland, Non-Ohmic dissipative regime in the superconducting transition of polycrystalline $Y_1Ba_2Cu_3O_x$, Phys. Rev. Lett. 60 (1988) 1061–1064.
[16] A.C. Wright, K. Zhang, A. Erbil, Dissipation mechanism in a high-Tc granular superconductor: applicability of a phase-slip model, Phys. Rev. B. 44 (1991) 863–866.
[17] C. Gaffney, H. Petersen, R. Bednar, Phase-slip analysis of the non-Ohmic transition in granular $YBa_2Cu_3O_{6.9}$, Phys. Rev. B. 48 (1993) 3388–3392.
[18] H.S. Gamchi, G.J. Russell, K.N.R. Taylor, Resistive transition for $YBa_2Cu_3O_{7-\delta}$-Y_2BaCuO_5 composites: influence of a magnetic field, Phys. Rev. B. 50 (1994) 12950–12958.
[19] A.G. Mamalis, S.G. Ovchinnikov, M.I. Petrov, D.A. Balaev, K.A. Shaihutdinov, D.M. Gohfeld, S.A. Kharlamova, I.N. Vottea, Composite materials on high-Tc superconductors and $BaPbO_3$, Ag basis, Phys. C Supercond. Its Appl. 364 (2001) 174–177.
[20] D.A. Balaev, A.G. Prus, K.A. Shaykhutdinov, D.M. Gokhfeld, M.I. Petrov, Study of dependence upon the magnetic field and transport current of the magnetoresistive effect in YBCO-based bulk composites, Supercond. Sci. Technol. 20 (2007) 495–499.
[21] D. Lopez, F. De la Cruz, Anisotropic energy dissipation in high-Tc ceramic superconductors: local-field effects, Phys. Rev. B. 43 (1991) 11478–11480.
[22] D. Lopez, R. Decca, F. De la Cruz, Anisotropic energy dissipation, flux flow and topological pinning in ceramic superconductors, Supercond. Sci. Technol. 5 (1992) S276–S279.
[23] D.A. Balaev, A.A. Bykov, S.V. Semenov, S.I. Popkov, A.A. Dubrovskii, K.A. Shaikhutdinov, M.I. Petrov, General regularities of magnetoresistive effects in the polycrystalline yttrium and bismuth high-temperature superconductor systems, Phys. Solid State. 53 (2011) 922–932.
[24] M. Prester, E. Babić, M. Stubičar, P. Nozar, Dissipation in a weak-link-limited superconductor as a problem of percolation theory, Phys. Rev. B. 49 (1994) 6967–6970.
[25] M. Prester, Current transfer and initial dissipation in high-superconductors, Supercond. Sci. Technol. 11 (1998) 333–357.
[26] D.A. Balaev, S.I. Popkov, S.V. Semenov, A.A. Bykov, E.I. Sabitova, A.A. Dubrovskiy, K.A. Shaikhutdinov, M.I. Petrov, Contributions from inter-grain boundaries to the magneto-resistive effect in polycrystalline high-t superconductors. the underlying reason of different behavior for YBCO and BSCCO systems. J. Supercond. Nov. Magn. 24 (2011) 2129–2136.
[27] V. Derevyanko, T. Sukhareva, V. Finkel, Y. Shakhov, Effect of temperature and magnetic field on the evolution of a vortex structure of the granular YBaCuO high-temperature superconductor, Phys. Solid State. 56 (2014) 649–658.
[28] J.E. Evetts, B.A. Glowacki, Relation of critical current irreversibility to trapped flux and microstructure in polycrystalline $YBa_2Cu_3O_7$, Cryogenics (Guildf). 28 (1988) 641–649.
[29] K.-H. Müller, D.N. Matthews, A model for the hysteretic critical current density in polycrystalline high-temperature superconductors, Physica C 206 (1993) 275–284.
[30] Y.J. Qian, Z.M. Tang, K.Y. Chen, B. Zhou, J.W. Qiu, B.C. Miao, Y.M. Cai, Transport hysteresis of the oxide superconductor $Y_1Ba_2Cu_3O_{7-x}$ in applied fields, Phys. Rev. B. 39 (1989) 4701–4703.
[31] S. Shifang, Z. Yong, P. Guoqian, Y. Daoq, An Z., C. Zuyao, Q. Yitai, K. Eiyan, Z. Qirui, The behaviour of negative magnetoresistance and hysteresis in $YBa_2Cu_3O_{7-\delta}$, Europhys. Lett. 6 (1988) 359–362.
[32] M. Celasco, A. Masoero, P. Mazzetti, A. Stepanescu, Evidence of current-noise hysteresis in superconducting $YBa_2Cu_3O_{7-\delta}$ specimens in a magnetic field, Phys. Rev. B. 44 (1991) 5366–5368.
[33] D. Daghero, P. Mazzetti, A. Stepanescu, P. Tura, A. Masoero, Electrical anisotropy in high-T c granular superconductors in a magnetic field, Phys. Rev. B. 66 (2002) 184514.
[34] C.A.M. dos Santos, M.S. da Luz, B. Ferreira, A.J.S. Machado, On the transport properties in granular or weakly coupled superconductors, Physica C 391 (2003) 345–349.
[35] N.D. Kuz'michev, Critical state of Josephson medium, JETP Lett. 74 (2001) 262–266.
[36] V.V. Derevyanko, T.V. Sukhareva, V.A. Finkel, Magnetoresistance hysteresis of granular $YBa_2Cu_3O_{7-\delta}$ high-temperature superconductor in weak magnetic fields, Tech. Phys. 53 (2008) 321–327.
[37] T.V. Sukhareva, V.a. Finkel', Hysteresis of the magnetoresistance of granular HTSC $YBa_2Cu_3O_{7-\delta}$ in weak fields, Phys. Solid State. 50 (2008) 1001–1008.
[38] T.V. Sukhareva, V.A. Finkel, Phase transition in the vortex structure of granular $YBa_2Cu_3O_{7-\delta}$ HTSCs in weak magnetic fields, J. Exp. Theor. Phys. 107 (2008) 787–793.
[39] D.A. Balaev, S.I. Popkov, E.I. Sabitova, S.V. Semenov, K.A. Shaykhutdinov, A.V. Shabanov, M.I. Petrov, Compression of a magnetic flux in the intergrain medium of a YBa2Cu3O7 granular superconductor from magnetic and magnetoresistive measurements, J. Appl. Phys. 110 (2011) 93918.
[40] D.A. Balaev, S.I. Popkov, S.V. Semenov, A.A. Bykov, K.A. Shaykhutdinov, D.M. Gokhfeld, M.I. Petrov, Magnetoresistance hysteresis of bulk textured $Bi_{1.8}Pb_{0.3}Sr_{1.9}Ca_2Cu_3O_x$ + Ag ceramics and its anisotropy, Phys. C 470 (2010) 61–67.
[41] D.A. Balaev, A.A. Dubrovskii, S.I. Popkov, D.M. Gokhfeld, S.V. Semenov, K.A. Shaykhutdinov, M.I. Petrov, Specific features in the hysteretic behavior of the magnetoresistance of granular high-temperature superconductors, Phys. Solid State. 54 (2012) 2155–2164.
[42] A. Altinkok, K. Kilic, M. Olutaş, A. Kilic, Magnetovoltage measurements and hysteresis effects in polycrystalline superconducting Y1Ba2Cu3O7−x/Ag in weak magnetic fields, J. Supercond. Nov. Magn. 26 (2013) 3085–3098.
[43] M.N. Kunchur, T.R. Askew, Hysteretic internal fields and critical currents in polycrystalline superconductors, J. Appl. Phys. 84 (1998) 6763–6767.
[44] G. Blatter, M.V. Feigel'man, V.B. Geshkenbein, A.I. Larkin, V.M. Vinokur, Vortices in high-temperature superconductors, Rev. Mod. Phys. 66 (1994) 1125–1388.
[45] K.A. Shaikhutdinov, D.A. Balaev, S.I. Popkov, M.I. Petrov, Mechanism of formation of a negative magnetoresistance region in granular high-temperature superconductors, Phys. Solid State. 51 (2009) 1105–1109.
[46] D.A. Balaev, S.I. Popkov, K.A. Shaikhutdinov, M.I. Petrov, D.M. Gokhfeld, Magnetoresistance of porous polycrystalline HTSC: effect of the transport current on magnetic flux compression in intergranular medium, Phys. Solid State. 56 (2014)

1542–1547.
[47] E. Altshuler, J. Musa, J. Barroso, A.R.R. Papa, V. Venegas, Generation of Jc (He) hysteresis curves for granular YBa2Cu3O7-δ superconductors, Cryogenics 33 (1993) 308–313.
[48] P. Mune, E. Govea-Alcaide, R.F. Jardim, Magnetic hysteresis of the critical current density of polycrystalline (Bi–Pb)–Sr–Ca–Cu–O superconductors: a fingerprint of the intragranular and intergranular flux trapping, Phycica C 354 (2001) 275–278.
[49] P. Mune, F.C. Fonseca, R. Muccillo, R.F. Jardim, Magnetic hysteresis of the magnetoresistance and the critical current density in polycrystalline YBa 2 Cu 3 O 7 − δ–Ag superconductors, Phys. C 390 (2003) 363–373.
[50] D.A. Balaev, S.V. Semenov, M.I. Petrov, Correlation between magnetoresistance and magnetization hysteresis in a granular high-Tc superconductor: impact of flux compression in the intergrain medium, J. Supercond. Nov. Magn. 27 (2014) 1425–1429.
[51] S.V. Semenov, D.A. Balaev, M.A. Pochekutov, D.A. Velikanov, Anisotropy of the magnetoresistive properties of granular high-temperature superconductors resulting from magnetic flux compression in the intergrain medium, Phys. Solid State. 59 (2017) 1291–1297.
[52] D.A. Balaev, S.V. Semenov, M.A. Pochekutov, Anisotropy of the magnetoresistance hysteresis in the granular superconductor Y-Ba-Cu-O at different magnetic-field and transport-current orientations, J. Appl. Phys. 122 (2017) 123902.
[53] A.D. Balaev, Y.V. Boyarshinov, M.M. Karpenko, B.P. Khrustalev, Automated magnetometer with superconducting solenoid, Prib. Tekh. Eksp. 3 (1985) 167.
[54] D.M. Gokhfeld, An extended critical state model: asymmetric magnetization loops and field dependence of the critical current of superconductors, Phys. Solid State. 56 (2014) 2380–2386.
[55] D.A. Balaev, D.M. Gokhfeld, A.A. Dubrovskiĭ, S.I. Popkov, K.A. Shaikhutdinov, M.I. Petrov, Magnetoresistance hysteresis in granular HTSCs as a manifestation of the magnetic flux trapped by superconducting grains in YBCO + CuO composites, J. Exp. Theor. Phys. 105 (2007) 1174–1183.
[56] D.A. Balaev, A.A. Dubrovskiĭ, K.A. Shaikhutdinov, S.I. Popkov, D.M. Gokhfeld, Y.S. Gokhfeld, M.I. Petrov, Mechanism of the hysteretic behavior of the magnetoresistance of granular HTSCs: the universal nature of the width of the magnetoresistance hysteresis loop, J. Exp. Theor. Phys. 108 (2009) 241–248.